Received: 16 February 2026 | Revised: 4 June 2026 | Accepted: 8 June 2026

DOI: 10.1002/ctm2.70722

CLINICAL AND TRANSLATIONAL MEDICINE Open Access

WILEY

RESEARCH ARTICLE

A living biobank of sarcoma patient-derived cell cultures reveals multi-omic and functional insights that capture disease heterogeneity

Stefanie Gijsels[1,2,3] | **Suzanne Fischer**[1,3] | **David Creytens**[3,4,5] | **Sándor Dedeyne**[1,3] | **Felix De Vuyst**[1,3] | **Cláudio Pinheiro**[1,3] | **Fleur Cordier**[3,4] | **Sarah-Lee Bekaert**[3,6,7] | **Nadine Van Roy**[3,6,7,8] | **Kaat Durinck**[3,6,7,8] | **Jarne Pauwels**[3,7,9] | **Kris Gevaert**[3,7,9] | **Pieter Mestdagh**[3,10] | **Jo Vandesompele**[3,10] | **Pekka Rappu**[11] | **Jyrki Heino**[11] | **An Hendrix**[1,3] | **Gabrielle H. van Ramshorst**[2,3] | **Gwen Sys**[3,12] | **Olivier De Wever**[1,3]

[1]Laboratory of Experimental Cancer Research, Department of Human Structure and Repair, Ghent University, Corneel Heymanslaan, Ghent, Belgium

[2]Department of Gastrointestinal surgery, Ghent University Hospital, Corneel Heymanslaan, Ghent, Belgium

[3]Cancer Research Institute Ghent, Ghent University, Corneel Heymanslaan, Ghent, Belgium

[4]Department of Pathology, Ghent University Hospital, Corneel Heymanslaan, Ghent, Belgium

[5]Research Foundation Flanders (FWO), Brussels, Belgium

[6]Paediatric Precision Oncology Lab, Ghent University, Corneel Heymanslaan, Ghent, Belgium

[7]Department of Biomolecular Medicine, Ghent University, Corneel Heymanslaan, Ghent, Belgium

[8]Centre for Medical Genetics, Ghent University Hospital, Corneel Heymanslaan, Ghent, Belgium

[9]VIB-UGent Center for Medical Biotechnology, VIB, Technologiepark-Zwijnaarde, Ghent, Belgium

[10]OncoRNALab, Department of Biomolecular Medicine, Ghent University, Corneel Heymanslaan, Ghent, Belgium

[11]Department of Life Technologies and InFLAMES Flagship, University of Turku, Turku, Finland

[12]Department of Orthopedics and Traumatology, Ghent University Hospital, Corneel Heymanslaan, Ghent, Belgium

CLINICAL AND TRANSLATIONAL MEDICINE
Open Access

Correspondence
Olivier De Wever, Universiteit Gent Vakgroep Structuur en Herstel van de Mens, Belgium.
Email: Olivier.dewever@ugent.be

Graphical Abstract

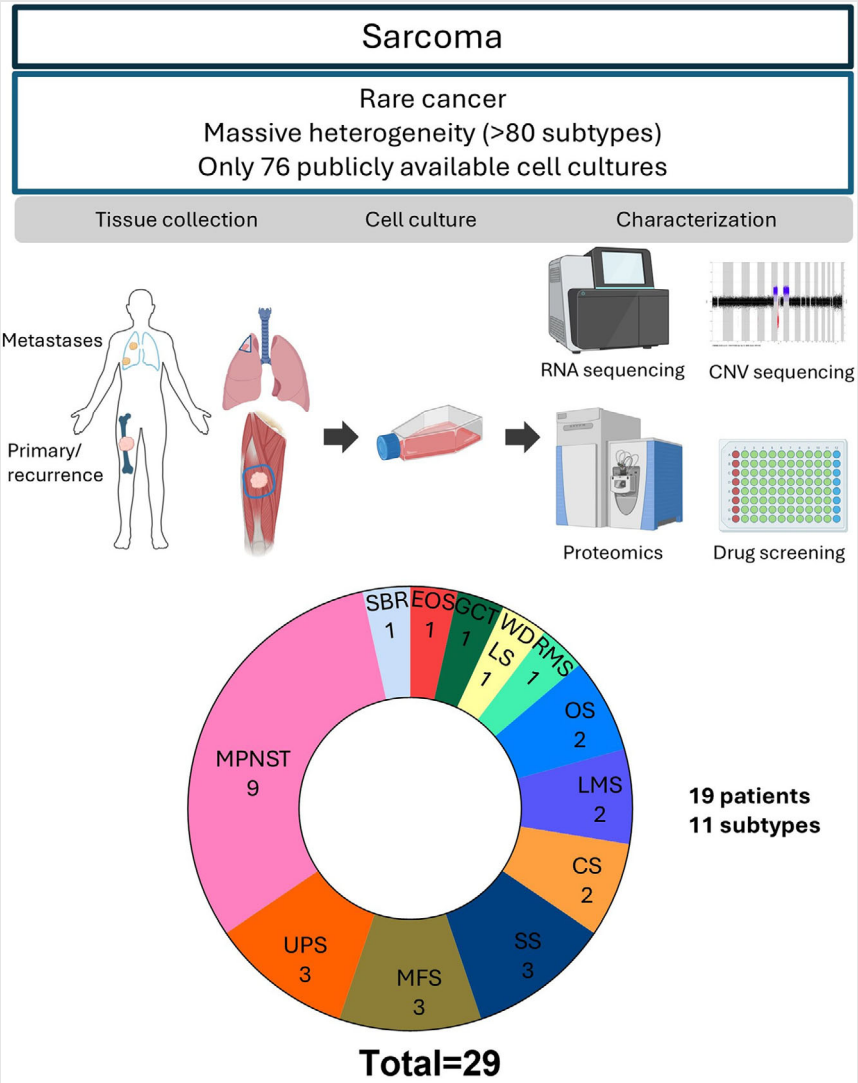

Preclinical models for sarcoma that preserve tumour biology are urgently needed to advance mechanistic understanding and functional precision oncology. 29 early-passage patient-derived sarcoma cell (PDC) cultures from 19 patients, representing 11 sarcoma subtypes were established and extensively characterized. This demonstrates that early-passage sarcoma PDCs capture lineage identity, tumour evolution and functional heterogeneity.

Received: 16 February 2026 | Revised: 4 June 2026 | Accepted: 8 June 2026

DOI: 10.1002/ctm2.70722

CLINICAL AND TRANSLATIONAL MEDICINE Open Access WILEY

RESEARCH ARTICLE

A living biobank of sarcoma patient-derived cell cultures reveals multi-omic and functional insights that capture disease heterogeneity

Stefanie Gijsels[1,2,3] | **Suzanne Fischer**[1,3] | **David Creytens**[3,4,5] | **Sándor Dedeyne**[1,3] | **Felix De Vuyst**[1,3] | **Cláudio Pinheiro**[1,3] | **Fleur Cordier**[3,4] | **Sarah-Lee Bekaert**[3,6,7] | **Nadine Van Roy**[3,6,7,8] | **Kaat Durinck**[3,6,7,8] | **Jarne Pauwels**[3,7,9] | **Kris Gevaert**[3,7,9] | **Pieter Mestdagh**[3,10] | **Jo Vandesompele**[3,10] | **Pekka Rappu**[11] | **Jyrki Heino**[11] | **An Hendrix**[1,3] | **Gabrielle H. van Ramshorst**[2,3] | **Gwen Sys**[3,12] | **Olivier De Wever**[1,3]

[1]Laboratory of Experimental Cancer Research, Department of Human Structure and Repair, Ghent University, Corneel Heymanslaan, Ghent, Belgium

[2]Department of Gastrointestinal surgery, Ghent University Hospital, Corneel Heymanslaan, Ghent, Belgium

[3]Cancer Research Institute Ghent, Ghent University, Corneel Heymanslaan, Ghent, Belgium

[4]Department of Pathology, Ghent University Hospital, Corneel Heymanslaan, Ghent, Belgium

[5]Research Foundation Flanders (FWO), Brussels, Belgium

[6]Paediatric Precision Oncology Lab, Ghent University, Corneel Heymanslaan, Ghent, Belgium

[7]Department of Biomolecular Medicine, Ghent University, Corneel Heymanslaan, Ghent, Belgium

[8]Centre for Medical Genetics, Ghent University Hospital, Corneel Heymanslaan, Ghent, Belgium

[9]VIB-UGent Center for Medical Biotechnology, VIB, Technologiepark-Zwijnaarde, Ghent, Belgium

[10]OncoRNALab, Department of Biomolecular Medicine, Ghent University, Corneel Heymanslaan, Ghent, Belgium

[11]Department of Life Technologies and InFLAMES Flagship, University of Turku, Turku, Finland

[12]Department of Orthopedics and Traumatology, Ghent University Hospital, Corneel Heymanslaan, Ghent, Belgium

Correspondence
Olivier De Wever, Universiteit Gent Vakgroep Structuur en Herstel van de Mens, Belgium.
Email: Olivier.dewever@ugent.be

Funding information
Cancer Research Institute Ghent; Stichting Tegen Kanker, Grant/Award Number: 2022-147; Kom op tegen Kanker, Grant/Award Number: A18/OC/0303; David Creytens was financially supported by a senior clinical research fellowship

Abstract

Background: Sarcomas are rare, diverse malignancies with limited therapeutic options and poor clinical outcomes. Preclinical models that preserve tumour biology are urgently needed to advance mechanistic understanding and functional precision oncology. We established and comprehensively characterized 29 early-passage patient-derived sarcoma cell (PDC) cultures from 19 patients, representing 11 sarcoma subtypes. Multi-region and multi-site sampling enabled generation of PDCs from spatially distinct areas of individual tumours and from matched primary, recurrent and metastatic lesions.

from the Research Foundation Flanders (FWO), Grant/Award Number: 1800725N

Methods: PDCs underwent genomic, transcriptomic and proteomic profiling alongside extracellular vesicle (EV) biomarker evaluation and phenotypic and drug-response assays.

Results: Copy-number variant (CNV) analysis revealed recurrent alterations affecting key regulators of cell cycle control and growth signalling. Bulk RNA-sequencing captured substantial inter- and intra-subtype heterogeneity. Proteomic and EV analyses recapitulated subtype- and site-specific differences. A functional drug screen of 38 clinically relevant and investigational agents identified both shared and divergent therapeutic vulnerabilities in the different PDCs.

Discussion: These results demonstrate that early-passage sarcoma PDCs can be regarded as biologically faithful and experimentally tractable models that capture lineage identity, tumour evolution and functional heterogeneity. Integrated multi-omic and functional profiling reveals therapeutic vulnerabilities not evident from genomic data only, supporting PDCs as valuable platforms for translational sarcoma research.

KEYWORDS
biobank, drug screening, functional assays, patient-derived cell cultures, sarcoma

Key points

- A PDC biobank that addresses a critical gap in sarcoma research.
- Investigation of intra-patient and inter-patient heterogeneity.
- Comprehensive characterization shows truthful recapitulation of sarcoma features.
- Functional assays highlight the importance of functional models in cancer research.

1 | INTRODUCTION

Sarcomas are rare malignant tumours of mesenchymal origin, comprising more than 80 histological subtypes that collectively account for only 4–5 new cases per 100 000 individuals per year.[1, 2] Despite their low incidence, sarcomas encompass an extraordinary degree of clinical, morphological and molecular heterogeneity, posing substantial challenges for diagnosis, prognostication and treatment. The overall 5-year survival rate remains approximately 60%, but outcomes vary widely across subtypes and decline sharply for aggressive, high-grade or metastatic disease.[2, 3] Therapeutic options remain limited, with doxorubicin-based chemotherapy continuing to serve as the first-line standard for most soft tissue sarcomas and few approved targeted therapies demonstrating broad or durable benefit. This persistent gap between molecular understanding and clinical progress underscores the urgent need for model systems that reflect sarcoma biology and can accelerate functional precision oncology.

Patient-derived cell (PDC) cultures represent a powerful but underutilized resource in this context. PDCs offer several advantages: they can be established rapidly, retain key morphological features of the parental tumour, support high-throughput functional assays and allow integrative genomic, transcriptomic and proteomic profiling.[4, 5] Across many cancer types, PDCs have contributed to drug discovery, mechanistic studies and biomarker identification. However, in sarcoma, PDC availability remains disproportionately limited. Compared to epithelial cancers, sarcomas are significantly underrepresented in public repositories.[6] A survey of major biobanks—including ATCC, DSMZ, ECACC, ICLC, IDAC and JCRB—reveals only 76 unique sarcoma cell cultures. Even the cell line information database Cellosaurus, containing 752 sarcoma entries, is heavily skewed toward paediatric subtypes like osteosarcoma (OS), rhabdomyosarcoma (RMS) and Ewing sarcoma (Table S1). Clinically important adult soft tissue sarcomas—including malignant peripheral nerve sheath tumour (MPNST), myxofibrosarcoma (MFS),

undifferentiated pleomorphic sarcoma (UPS) and synovial sarcoma (SS)—are sparsely represented or absent. This imbalance severely restricts opportunities to study sarcoma biology, investigate tumour evolution and identify therapeutic vulnerabilities across the disease spectrum.

Genomic data alone have also proven insufficient to guide therapy in most sarcoma types.[7] While translocation-driven sarcomas exhibit relatively simple karyotypes, the majority of adult soft tissue sarcomas harbour complex and highly unstable genomes.[8] Mutation analyses and copy number variant (CNV) profiling are increasingly used in clinical diagnostics, yet their predictive value for treatment response remains limited.[9] Notably, even comprehensive genomic characterization fails to capture functional properties such as drug sensitivity, invasive potential and adaptive cell-state transitions. These limitations reinforce the need for functional model systems that reflect both tumour-intrinsic molecular programs and their phenotypic consequences.

Large-scale initiatives such as the Genomics of Drug Sensitivity in Cancer (GDSC) project and Sarcoma_CellMinerCDB have begun to address these gaps by cataloguing drug responses across existing sarcoma cell lines.[10, 11] However, these collections rely heavily on extensively passaged lines that exhibit substantial genomic drift and may no longer represent the primary disease.[12, 13] Furthermore, many rare or clinically aggressive sarcoma subtypes remain unmodeled. Studies focussing on early-passage PDCs—where lineage identity, genomic architecture and functional traits are still closely preserved—remain scarce, but are important to further advance understanding of sarcoma.[14, 15] Therefore, there is a need for more comprehensive, multi-omic functional characterization studies across diverse sarcoma subtypes.

To address this critical unmet need, we established a panel of early-passage sarcoma PDC cultures representing 11 histologic subtypes. These cultures include multiple spatially distinct samples from individual tumours and matched sets from primary, recurrent and metastatic lesions, enabling the interrogation of both inter-patient and intra-patient heterogeneity. Using an integrated pipeline combining histopathology, CNV sequencing, transcriptomics, proteomics, extracellular vesicle (EV) profiling, morphological phenotyping and high-throughput drug sensitivity screening, we demonstrate that early-passage PDCs preserve subtype-specific molecular programs while revealing unanticipated functional diversity. Across the cohort, we identify both shared vulnerabilities—such as sensitivity to trabectedin, microtubule-targeting agents and PI3K–mTOR inhibitors—and clinically relevant subtype- or stage-specific behaviours, including mesenchymal plasticity and progression-linked drug sensitivities.

Together, these findings establish early-passage sarcoma PDCs as clinically meaningful and experimentally tractable models that can enhance precision oncology efforts by capturing the complex molecular heterogeneity and therapeutic susceptibilities of human sarcomas.

2 | METHODOLOGY

2.1 | Collection of tumour samples

Patients with suspected sarcoma were included after written informed consent (EC 2018/0080 and EC/2019/0178). During surgical procedures, fresh tumour tissue was collected according to the earlier published protocol.[16] The tissue was collected in a sterile fashion in the operating theatre and was subsequently transported to the lab in pre-heated culture medium. All patients were diagnosed with sarcoma before tumour resection by an expert sarcoma pathologist (DC), except for one that was diagnosed with giant cell tumour.

For the sample collection of the SAR183, SAR186 and SAR187, multiple samples were collected at different locations within the tumours, in collaboration with the pathologist (Supplementary Figure 1).

2.2 | Initiation of cell cultures

Tissue pieces of 0.5–2 cm^3 were cut into smaller pieces of 1–2 mm^3 and processed with 2.5 mL of 250 U/mL collagenase II solution (cat. no. 17101015, Fischer Scientific) and 2.5 mL of 0.2 mg/mL DNase I solution (cat. no. A3778.0010, VWR) according to the GentleMACS Dissociator TM (Miltenyi Biotec) tumour digestion protocol. The single-cell suspension was filtered through a 100 μm cell strainer (cat. no. 352360, Corning) and the lysate centrifuged at 300 RCF for 5 min. After removal of the supernatant, the pellet was resuspended in full medium (see below) and seeded in a 6-well plate or T25 flask. If the cell pellet was red after centrifugation, the pellet was first resuspended in erythrocyte lysis buffer and incubated for maximum 10 min. After addition of full medium, the suspension was centrifuged again, resulting in a white pellet. This pellet was then resuspended in full medium and seeded into a 6-well plate.

All cells were cultured in either DMEM (cat. no. 41965062, Fischer Scientific) or RPMI (cat. no. 12027599, Fischer Scientific), both supplemented with 10% Fetal bovine serum (FBS) (cat. no. P30-3306, Pan Biotech) and 100 IU/mL penicillin and 100 mg/mL streptomycin (cat. no. 15070063, ThermoFisher) (Table S3). All cultures were incubated at 37°C in a 5% CO_2 humidified atmosphere and monthly tested for Mycoplasma with the Mycoalert

Mycoplasma Detection Kit (cat. no. LT07-318, Lonza). All human cell cultures were authenticated using a 16-Marker STR Profile test (Eurofins). Cells were passaged at 80% confluence using a buffer solution with 5% glucose and trypsin-EDTA (0.05%) (cat. no. 11580626, Fischer Scientific).

2.3 | Identification of cell cultures in literature

A search in Cellosaurus was performed, that included the word 'sarcoma', 'solitary fibrous tumour', 'MPNST', 'malignant peripheral nerve sheath tumour', 'IMT', 'Inflammatory myofibroblastic tumour', 'Desmoplastic small round cell tumour' and 'malignant fibrous histiocytoma'. This was repeated in the cell culture biobanks of DSMZ, ATCC, ECACC, ICLC, IDAC and JCRB.

2.4 | Drug sensitivity screening

Cells were seeded in a 384 well white with clear bottom microplate (cat. no. CLS3544, Corning), at a density that was determined beforehand (Table S2) in 40 µL full medium. One day after seeding, 40 µL of full medium containing the therapies was added to the seeded cells, to reach final concentrations of 1, 10 and 100 nM. All conditions were tested in triplicates of the same seeding. After 6 days, viability of the cells was determined using CellTiter-Glo® 2.0 Cell Viability Assay (cat. no. G9243, Promega) according to the manufacturer's instructions. Read-out was performed using the Synergy HTX plate reader (BioTek). The application of DSS for assessment of sensitivity to certain treatments does not allow interpretation of variability between replicates, but does provide an overview of relative drug sensitivities across cell cultures and therapies.

Drug sensitivity scores were calculated with RStudio (Posit software, version 2024.12.1) using the DSS package.[17] A hierarchical cluster analysis was performed using RStudio with agglomerative nesting, Euclidian metric and ward linkage method.

2.5 | Clonogenicity assay

Cells were seeded in a 12-well flat bottom plate (cat. no. A18146, Novolab) at concentrations of 125, 250, 500, 1000 and 2000 cells/well in triplicate in 500 µL of full medium. Consecutively, 500 µL of conditioned medium of the same cell culture was added, which was prepared by collecting medium of a confluent flask and centrifugation at 300 g for 5 min. The cultures were kept for at least 6 doubling times, with weekly medium changes with a 1/1 ratio of fresh medium and conditioned medium. After 6 doubling times or a maximum of 3 weeks, all cultures were stained using crystal violet and colonies were manually counted.

2.6 | Invasion assay

Cells were seeded at 4000 cells/well in a 96-well ULA U-bottom plate (cat. no. CLS7007, Corning), allowing the formation of spheroids. 48 h after seeding, spheroids were transported to 500 µL of collagen type I gel (1 mg/mL) (cat. no. ALX-522-435, Enzo Life Sciences) in a 24-well flat bottom plate and cultured in full DMEM for 4 days. Imaging was performed at day 0 and day 4 using the Cytation 5 imaging multimode reader (BioTek) and Z-stacking in 5 layers. Images were analysed using ImageJ. The area of the spheroids was calculated on Day 0, and was subtracted from the total invaded area on Day 4.

2.7 | Morphology

Cells were seeded in 6-well flat-bottom plates at a density of 10 000 cells/well in 3 mL of full medium. After reaching confluence of 50%, culture medium was removed and cells were washed with preheated phosphate buffered saline (PBS) (cat. no. 11540546, Gibco) before staining with CellMask plasma membrane stain (cat. no C10045, Invitrogen) in preheated medium, according to the manufacturer's protocol. After 10 min of incubation at 37°C, the solution was removed and the cells were washed three times with PBS before imaging. Imaging was performed using the Cytation 5 imaging multimode reader (BioTek) using the RFP channel. Per well, three pictures at 10× magnification were taken. Morphology of the cells was then analysed with ImageJ, calculating the area, perimeter, circularity and roundness of the cells. Based on those parameters, plots were created in ClustVis.[18]

2.8 | RNA sequencing

Cells were cultured in 6-well flat-bottom plates (cat. no. 391-8036, Fischer Scientific) in triplicate. At 80% confluence, the cells were collected. Medium was aspirated, followed by addition of 700 µL QIAzol lysis reagent (cat. no. 79306, Qiagen) and scraping of the cells. The cell lysate was collected in 1.5 mL RNAse-free eppendorfs (cat.no. A14934, Novolab), vortexed thoroughly and stored in -80°C upon further use.

RNA was extracted using the miRNeasy kit (cat. no. 217084, Qiagen) according to the manufacturer's instructions. RNA-seq libraries were prepared from purified RNA using the QuantSeq 3' mRNA-Seq Library Prep Kit FWD for Illumina (cat. no. 139.96, Lexogen), starting from 27.5 ng RNA that was treated with Heat-Labile Double Strand-specific DNase (Arcticzymes). The individual libraries were quantified by qPCR using the KAPA Library Quantification Kit (Roche) and equimolarly pooled. The pool concentration was measured with Qubit, and sequencing was carried out at a concentration of 1.4 pM with 1% PhiX on a NextSeq 500 (Illumina) (NextSeq software v.4.0.1) using a high-output 1 × 75 run. Reads were mapped to the human genome using Tophat and gene expression counts were generated using HTSeq.

Normalization and differential expression analysis was performed using the DeSEQ2 package in RStudio. PCA plots were created after variance stabilization in DeSEQ2 using the top 500 differentially expressed genes. Gene set enrichment analysis was performed using the fgsea package and hallmark gene set from the Human Molecular Signatures Database (MSigDB).[19] A p value of 0.001 was applied as significance level.

2.9 | CNV sequencing

gDNA was isolated from cryopreserved tissue and cell cultures using the QiaCube robot and QiaAmp DNA mini kit (Qiagen) according to the manufacturer's instructions.

gDNA was analysed using sWGS on the Novaseq 6000 (Illumina Inc.), starting from 200 ng input of gDNA according to the manufacturer's instructions. Using a bin size of 100 kb, the R-Bioconductor package QDNAseq was applied to visualize the DNA copy-number profile and call genomic aberrations.[20] An amplification was called at a Z-score of more than 0.35, a homozygous loss was called at a Z-score of -2 or lower and a heterozygous deletion was called at a Z-score between -0.35 and -2. A non-significant loss was called at a Z-score between -0.1 and -0.35. All profiles were visualized using the online tool Vivar.[21]

Each genome profile was manually checked for aberrations. Genes with significant amplifications or deletions were cross referenced with OncoKB to determine whether they were known oncogenes or tumour suppressor genes.[22, 23] Heatmaps were constructed in Graphpad Prism for Windows version 8.4.3 (GraphPad Software, www.graphpad.com). Comparison between CNV profiles was performed with the CNpare package in RStudio.[24]

2.10 | Proteomics cell cultures

Cells were cultured in T182.5 cm^2 culture flasks. Upon collection, cells were detached using trypsin-EDTA (0.05%) (cat. no. 11580626, Fischer Scientific) and centrifuged at 300 g for 5 min. Subsequently, three wash steps were performed using sterile phosphate-buffered saline (Gibco, cat. no. 11540546) with centrifugation steps in between and the samples were divided over three different 1.7 mL Eppendorf tubes. The cell pellets were cryopreserved at -80°C until further use. Cell pellets (n = 24) were lysed and sonicated. 100 µg of protein from each sample was digested using the S-Trap Mini protocol (Protifi) according to the manufacturer's instructions. Peptide concentrations were measured using a Lunatic instrument (Unchained Labs), and 500 ng of peptides per sample were subjected to LC–MS/MS analysis on an Orbitrap Fusion Lumos mass spectrometer. Raw data files were processed using DIA-NN software (v1.8.2) and searched against the human proteome database (January 2023 release; 20 594 protein sequences). Trypsin was specified as the proteolytic enzyme, allowing up to one missed cleavage. Oxidation of methionine and protein N-terminal acetylation were included as variable modifications, while cysteine carbamidomethylation was set as a fixed modification. Protein quantification was performed using MaxLFQ values after removal of low-scoring precursors.

2.11 | EV isolation from cell-conditioned medium

Preparation and collection of cell culture conditioned medium (CCM) was performed according to the previously validated protocol described by Van Deun et al.[25–28] The protocol has been validated extensively, and demonstrated a consistently high yield of EV preparations with minimal contamination.[25–27] In brief, CCM was prepared from cells grown at 60%–80% confluency in seven multilayer culture flasks with three layers (cat. no. 10272721, Corning). Cells were washed once with serum-free (SF) medium, followed by two washing steps with 0.5% EDS supplemented medium. Flasks were incubated at 37°C in 5 or 10% CO_2 for 24 h. After 24 h CM was collected and centrifuged for 10 min at 300 × g at 4°C. The supernatant was filtered using a 0.45 µm cellulose acetate filter (cat. no. 734–5064, VWR International) and CM was concentrated up to 1 mL using a 10 kDa Centricon Plus-70 centrifugal unit at 4°C (cat. no. UFC701008, Merck Life Science). Concentrated CCM was stored at -80°C until further use.

EVs were separated from CCM via top-down OptiPrep density gradient ultracentrifugation (DGUC) as previously

described.[25, 28] In short, a discontinuous iodixanol gradient was prepared by layering 4 mL of 40%, 4 mL of 20%, 4 mL of 10% and 3.5 mL of 5% iodixanol on top of each other in a 16.8 mL open top polyallomer tube (cat. no. 337986, Beckman Coulter). One millilitre of CCM sample was overlaid on top of the gradient, followed by 18 h ultracentrifugation at 100 000 × *g* and 4°C using a SW32.1 Ti rotor (Beckman Coulter). Afterwards, 16 DGUC fractions of 1 mL were collected from the top of the gradient (EV-enriched fractions 9 and 10 - corresponding to 1.09–1.11 g/mL densities) and kept. DGUC fractions were collected and diluted to 15 mL with PBS, followed by a 3 h ultracentrifugation at 100 000 × *g* and 4°C using a SW32.1 Ti rotor. Resulting pellets were resuspended in 100 µL PBS and stored at -80°C until further use.

We have submitted all relevant data of our experiments to the EV-TRACK knowledgebase (EV-TRACK ID: EV250139).[29]

2.12 | Proteomics EVs

Samples were processed for liquid-chromatography tandem mass spectrometry (LC-MS/MS) by filter-aided sample preparation (FASP) as previously described.[30, 31] The FASP-digested peptides were acidified with 1% trifluoroacetic acid to a pH of 2–3, followed by desalting as described.[32] The desalted and dried peptides were dissolved in 0.1% formic acid for LC-MS analysis. The peptide samples were analysed by a nanoflow HPLC system (Easy-nLC1200, Thermo Fisher Scientific) coupled to Orbitrap Exploris Lumos mass spectrometer (Thermo Fisher Scientific) equipped with a high-field asymmetric waveform ion mobility spectrometry (FAIMS) device between a nano-electrospray ionization source and the mass spectrometer. Compensation voltages of -40 V and -60 V were used. Peptides were first loaded on a trapping column and then separated inline on a 15 cm C18 column (75 µm × 15 cm, ReproSil-Pur 3 µm 120 Å C18-AQ, Dr. Maisch HPLC GmbH) with a 120-min 2-step gradient consisting of solvents A (0.1% formic acid) and solvent B (acetonitrile/water (95:5(v/v)) with 0.1% formic acid) from 5 to 21% B in 62 min, from 21% to 36% B in 48 min, from 36% to 100% in 5 min and held at 100% B for 5 min. All samples were analysed by data independent acquisition (DIA), in which each cycle consisted of a full scan from 345 to 1005 m/z at a resolution of 120 000, maximum injection time of 50 ms and normalized automatic gain control (AGC) target of 300%. DIA MS2 scans were employed for all DIA scans at a resolution of 30 000, normalized AGC target 2000%, maximum injection time of 52 ms and 30 windows of variable window scheme with an overlap of 1 m/z covering m/z range from 350 to 1000.

DIA data was processed with Spectronaut software (version 19.0, Biognosys) using directDIA with FASTA files of universal contaminant proteins[33] and human uniprot reference proteome including isoforms (release 2024_3). Carbamidomethyl (C) was used as a fixed modification, and acetylation (protein N-terminus) and oxidation (M) were set as variable modifications. Maximum of two missed cleavages were allowed. PSM, peptide and protein group FDR thresholds of pulsar search/identification were set to 0.01. Cross-run normalization using local normalization strategy based on a RT dependent local regression model.[34] Only the peptides identified in all runs were used as a background in normalization. Quantitation was done in MS2 level measuring peak areas.

3 | RESULTS

3.1 | Establishment and characterization of early-passage sarcoma PDC cultures

3.1.1 | Establishment

In total, 29 different patient-derived cell (PDC) cultures were initiated, from 19 different patients (Figure 1, Table 1, Supplementary Figure 2). Eleven different types of sarcomas were used to initiate the cell cultures. These included high-grade MPNST, UPS, high-grade MFS, SS, carcinosarcoma (CS), high-grade leiomyosarcoma (LMS), osteosarcoma (OS), spindle-cell rhabdomyosarcoma (RMS), well-differentiated liposarcoma (LPS), extraskeletal osteosarcoma (EOS) and sarcoma with BCOR alterations (SBR). Additionally, one tenosynovial giant cell tumour (GCT) sample was included as the culture had already been initiated from the biopsy sample before the diagnosis was known. All patient data was meticulously updated along the patients' treatment course, including previously administered treatments and survival. In this patient cohort, 11 females and eight males were present with a median age of 55 (IQR 28–65). Median overall survival was 83 months, with 11 out of 19 patients still alive in August 2025. Thirteen samples were treatment naïve at the moment of surgery. The majority of treated patients received a combination of anthracyclines and ifosfamide or the protocol by the European and American Osteosarcoma (EURAMOS protocol) (Table 1). Nineteen samples originated from primary tumours, six were of metastatic origin and four were collected from a local recurrence (Figure 1B). In three patients, multiple samples were collected and used for PDC culture (Supplementary Figure 1). In patient TBB-S-044, a MPNST, samples were collected from multiple regions in the primary tumour and local recurrence, with one additional sample from a lung

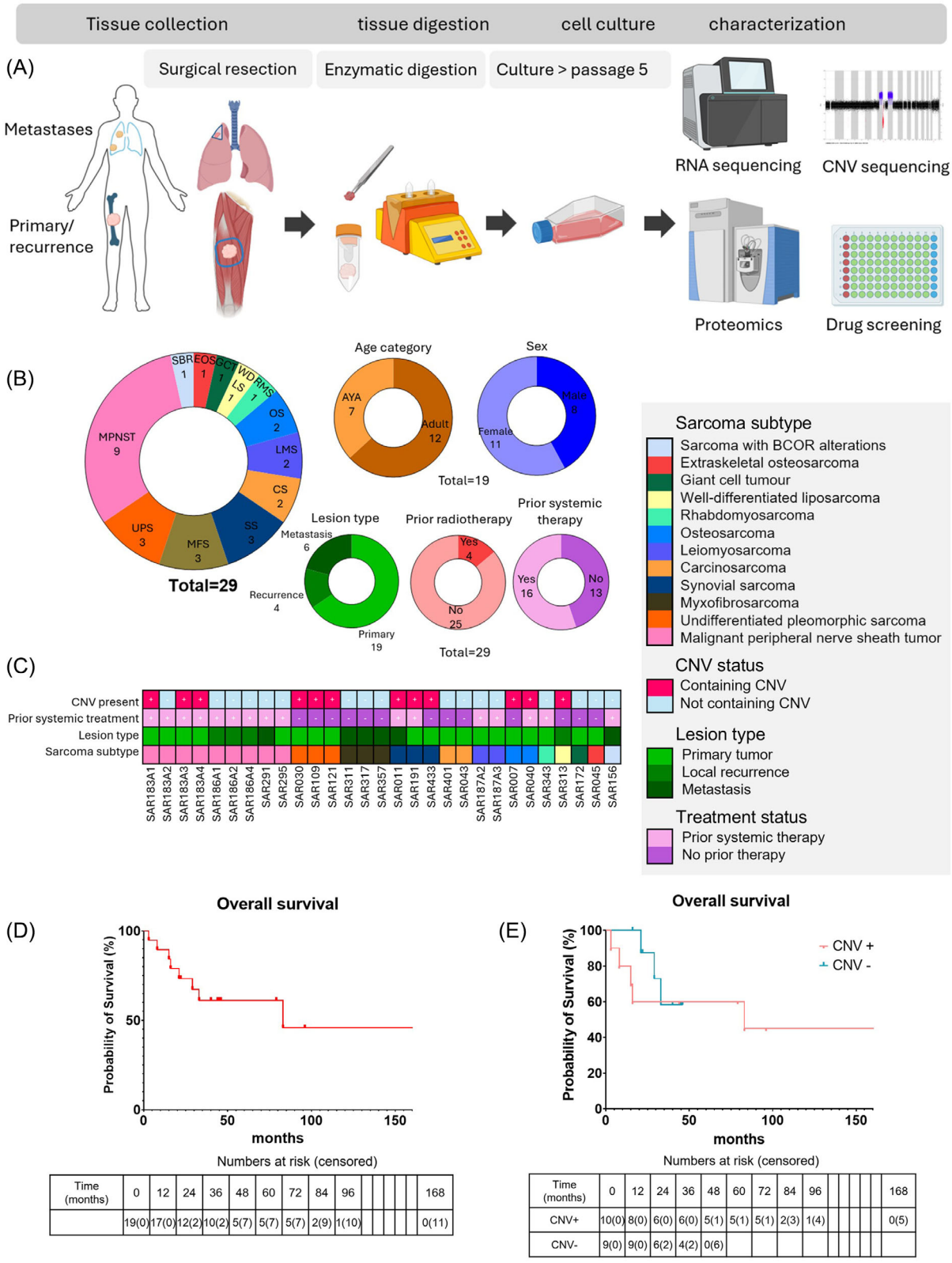

Time (months)	0	12	24	36	48	60	72	84	96	168
	19(0)	17(0)	12(2)	10(2)	5(7)	5(7)	5(7)	2(9)	1(10)	0(11)

Time (months)	0	12	24	36	48	60	72	84	96	168
CNV+	10(0)	8(0)	6(0)	6(0)	5(1)	5(1)	5(1)	2(3)	1(4)	0(5)
CNV-	9(0)	9(0)	6(2)	4(2)	0(6)					

FIGURE 1 Overview of PDC experimental procedures and associated clinical data. (A) Overview of experimental pipeline and procedures. (B and C) Overview of all established cultures with associated clinical parameters. (D) Survival analyses of all patients with numbers at risk and censored data. (E) Survival analyses of patients with and without copy number variations with numbers at risk and censored data. A log-rank (Mantel–Cox) test revealed no significant difference between the patients from whom PDCs with and without CNV were derived, with a mean overall survival of 83 months in the patients that gave rise to PDCs carrying CNVs, and undefined median survival in the patients that gave rise to PDCs without CNVs. CNV+ = cultures containing copy number variations, CNV- = cultures not containing copy number variations.

TABLE 1 Overview of sarcoma cell cultures.

Patient ID	Culture name	Sarcoma subtype	Disease stage	Prior treatment	Vital status	Sex	Age (y)
TBB-S-050	SAR007	Osteosarcoma	Primary tumour	–	Deceased	F	66
TBB-S-010	SAR011	Synovial sarcoma	Metastasis	Doxorubicin + ifosfamide, trabectedin	Deceased	F	66
TBB-S-045	SAR030	Undifferentiated sarcoma, pleomorphic	Primary tumour	–	Alive	F	70
TBB-S-247	SAR040	Osteosarcoma	Primary tumour	EURAMOS	Alive	M	24
TBB-S-250	SAR043	Carcinosarcoma	Primary tumour	–	Deceased	F	49
TBB-S-047	SAR045	Extraskeletal osteosarcoma	Primary tumour	–	Deceased	M	24
TBB-S-087	SAR109	Undifferentiated sarcoma, pleomorphic	Primary tumour	–	Deceased	M	76
TBB-S-099	SAR121	Undifferentiated sarcoma, pleomorphic	Primary tumour	–	Deceased	M	62
TBB-S-058	SAR156	Sarcoma with BCOR genetic alterations	Metastasis	VDC/IE	Deceased	M	46
TBB-S-044	SAR183A1	MPNST	Primary tumour	Anthracycline + ifosfamide	Deceased	F	31
	SAR183A2						
	SAR183A3						
	SAR183A4						
	SAR186A1		Local recurrence	Anthracycline + ifosfamide Radiotherapy			
	SAR186A2						
	SAR186A4						
	SAR291		Metastasis	Anthracycline + ifosfamide			
TBB-S-155	SAR187A2	Leiomyosarcoma	Primary tumour	Anthracycline + DTIC	Alive	F	65
	SAR187A3						
TBB-S-161	SAR191	Synovial sarcoma	Primary tumour	Anthracyclin + ifosfamide Radiotherapy	Alive	F	19
TBB-S-028	SAR295	MPNST	Primary tumour	Anthracycline + ifosfamide	Alive	M	25
TBB-S-052	SAR311	Myxofibrosarcoma	Metastasis	–	Alive	M	55
	SAR317						
	SAR357						
TBB-S-229	SAR313	Well-differentiated liposarcoma	Local recurrence	–	Alive	M	33
TBB-S-031	SAR343	Rhabdomyosarcoma	Primary tumour	IVADO	Alive	F	65
TBB-S-342	SAR433	Synovial sarcoma	Primary tumour	–	Alive	F	21
TBB-S-146	SAR172	Giant cell tumour	Primary tumour	–	Alive	F	55
TBB-S-316	SAR401	Carcinosarcoma	Primary tumour	–	Alive	F	65
–	SW1353	Chondrosarcoma	Primary tumour	–	Deceased	F	N/A

Note: In patients TBB-S-044 and TBB-S-155, multiple samples were collected of single tumours. In patient TBB-S-052, samples of three different metastases were collected at two different timepoints. Age is the age of patients at the moment of surgery.Abbreviations: EURAMOS: combination treatment containing cisplatin, doxorubicin and methotrexate; IVADO: combination treatment containing ifosfamide, vincristine, actinomycin D and doxorubicin. MPNST: malignant peripheral nerve sheath tumour; VDC/IE: combination treatment containing vincristine, doxorubicin, cyclophosphamide, ifosfamide, etoposide.

metastasis. In patient TBB-S-155, a LMS, samples were collected from three macroscopically different regions of the primary tumour, of which two separate cell cultures could be initiated. In patient TBB-S-052, three different MFS metastases were collected throughout the disease course, and all successfully generated PDC cultures. The majority of PDC cultures adopted a spindle-shaped morphology, which was also present in the original histology of the patient samples (Figures S2 and S3). Hematoxylin/Eosin evaluation of the cell pellets from suspended cultures showed a typical rounded morphology, with cells displaying relatively large nuclei. This appearance is consistent with an increased nuclear-to-cytoplasmic ratio, a feature commonly observed in cancerous cell populations (Supplementary Figure 3).

3.1.2 | Genetic characterization

CNV sequencing revealed the presence of copy number alterations in 12 out of 29 cell cultures (Figure 1C, Table S3). The majority of cultures showed complex genomes with presence of multiple amplifications and chromosomal losses (Supplementary Figure 4). A set of genes that are frequently affected in sarcoma was selected based on OncoKB, and cell cultures were compared based on these genes (Figure 2B). The most frequent CNVs identified are losses of the cell cycle inhibitors *CDKN2A* and *CDKN2B*, that were present in different sarcoma subtypes. Loss-of-function alterations in NF1 are a defining feature of NF1-associated MPNSTs and represent the most frequent genetic events in sporadic MPNSTs, where they commonly co-occur with deletion of the tumour suppressor gene SUZ12.[35] Accordingly, all MPNST PDCs harbouring CNVs exhibited concurrent loss of NF1 and SUZ12 on chromosome 17q (Supplementary Figure 4). The most complex profiles were found in the UPS (SAR121, SAR109 and SAR030), which show a multitude of CNVs involving oncogenes and tumour suppressor genes including *BRCA2, TP53, CDKN2A, CDKN2B, RB1* (Figure 3E, Supplementary Figure 4). All SS (SAR011, SAR191 and SAR433) shared a similar amplification on chromosome 17 that, despite harbouring no known relevant oncogenes, may play a role in tumourigenesis (Supplementary Figure 4).[36]

3.1.3 | Transcriptomic analysis

Principal component analysis (PCA) of transcriptomes from the 29 PDC cultures revealed distinct clustering driven largely by sarcoma subtype (Figure 2A). SS PDC (SAR011, SAR191, SAR433) formed a tight and clearly separated cluster, consistent with their distinct fusion-driven and transcriptionally coherent neural-crest/myogenic identity. MFS PDC (SAR311, SAR317 and SAR357) and UPS PDC (SAR030, SAR109 and SAR121) each formed discrete clusters, reflecting their fibroblastic lineage (MFS) versus dedifferentiated, lineage-erased state (UPS). LMS cultures (SAR187A2 and A3) clustered closely together, consistent with preserved smooth-muscle differentiation, whereas OS (SAR007 and SAR040) and CS (SAR401 and SAR043) samples occupied intermediate regions of PCA space, reflecting mixed or partially retained lineage programs. MPNST (SAR183, SAR186, SAR291 and SAR295) cultures predominantly remained separated along PC1 and were distinctly separated along PC2 from SS, MFS and UPS underscoring their differential lineage-of-origin. The variation along PC1 may align with the biological context of the samples, which are derived from a primary tumour (SAR183), a local relapse, (SAR186) and a distant lung metastasis (SAR291) all originating from the same patient and each representing distinct stages of tumour evolution. Additional single-cultured subtypes also mapped to distinct PCA positions consistent with their differential biology: RMS (rhabdomyoblastic lineage), liposarcoma (adipogenic differentiation), tenosynovial GCT (osteoclastic/stromal signature), EOS (mixed osteogenic–fibroblastic identity) and a BCOR-altered sarcoma (unique chromatin-driven transcriptional pattern). These entities did not cluster with the major sarcoma groups, further demonstrating that PCA captures biologically meaningful transcriptional variation across diverse mesenchymal tumour lineages. Furthermore, a complementary PCA incorporating two epithelial cancer cell lines underscores the lineage differences captured by PC1 (Supplementary Figure 5). Hierarchical clustering of the transcriptomic profiles largely reproduced the subtype-driven structure observed in the PCA (Figure 2C). The majority of PDC from SS, MFS and UPS formed coherent clusters with strong within-subtype correlations and clear separation from one another. As expected, MPNST cultures formed multiple distinct clusters, more consistent with their origin from primary, recurrent and metastatic lesions. Other subtypes such as RMS, liposarcoma, GCT, EOS and the BCOR-altered sarcoma occupied isolated positions. Overall, both analyses demonstrate that lineage of origin and tumour progression stage are major drivers of transcriptomic heterogeneity in the sarcoma PDC panel. Despite this intra- and inter-subtype variation, ssGSEA revealed some strikingly homogeneous pathway activity profiles across a majority of cultures, with consistently high enrichment of *MYC* targets, *TGF-β* signalling, oxidative phosphorylation and *mTORC1* signalling, suggesting shared therapeutic vulnerabilities (Figure 2B). Furthermore, gene set enrichment analysis comparing PDCs containing CNVs to PDCs not containing CNVs showed

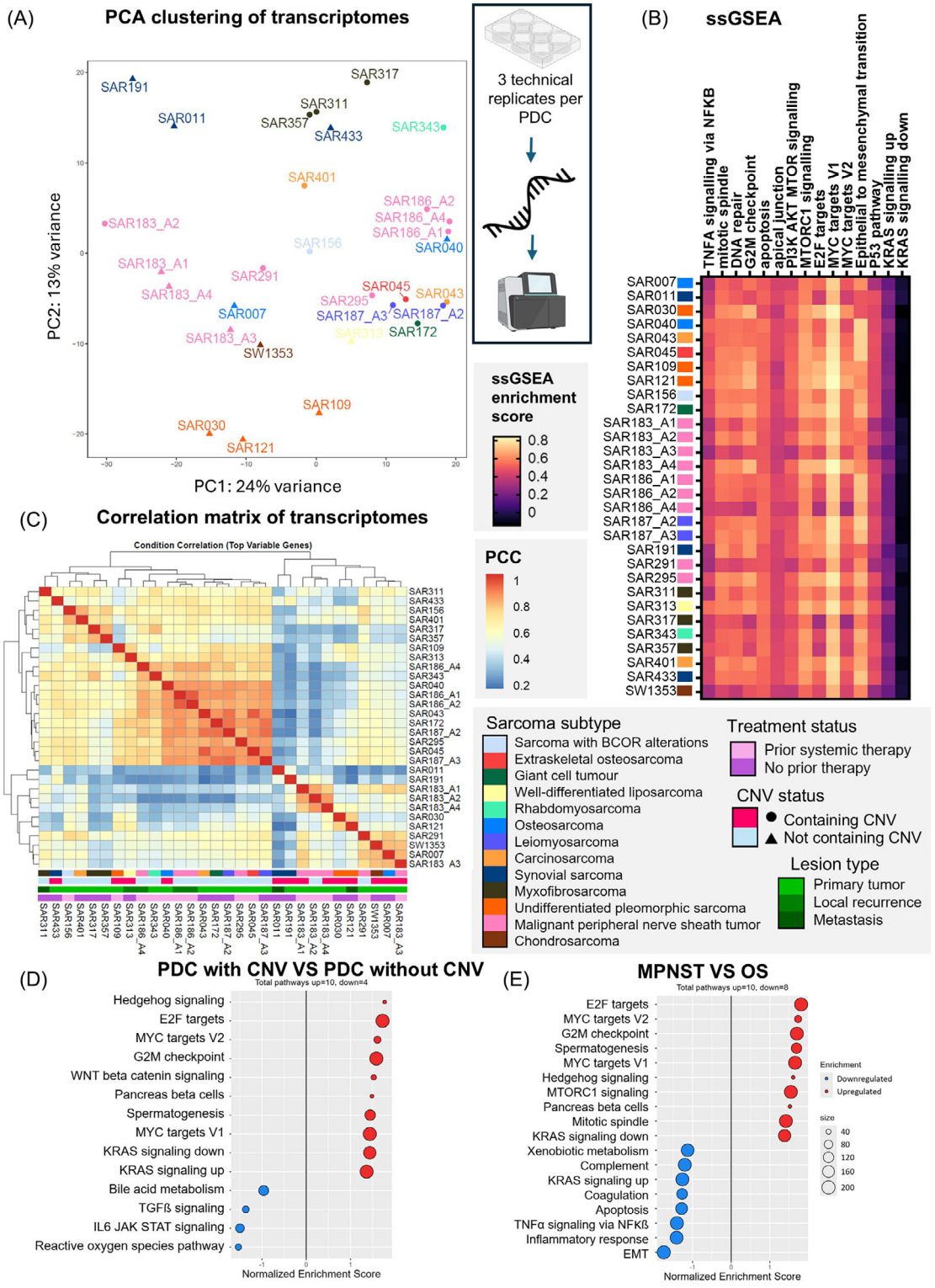

FIGURE 2 Bulk RNA sequencing results from all PDCs. (A) PCA plot based on bulk RNA sequencing based on the top 2000 genes after variance stabilising reveals clustering both within subtypes and within patients. (B) Single sample GSEA based on bulk RNA sequencing shows homogenously up- and downregulated pathways in PDCs of multiple sarcoma subtypes. (C) Correlation matrix of transcriptomes based on the top 1000 most variable genes applying Pearson correlation. (D) GSEA based on the Hallmarks dataset from MSigDB comparing PDC with CNVs to PDC without CNVs. The top 10 most significant pathways are shown. A *p*-value of 0.001 was applied for significance. (E) GSEA comparing MPNST PDC to OS PDC. A *p*-value of 0.001 was applied for significance. PCC = Pearson Correlation Coefficient.

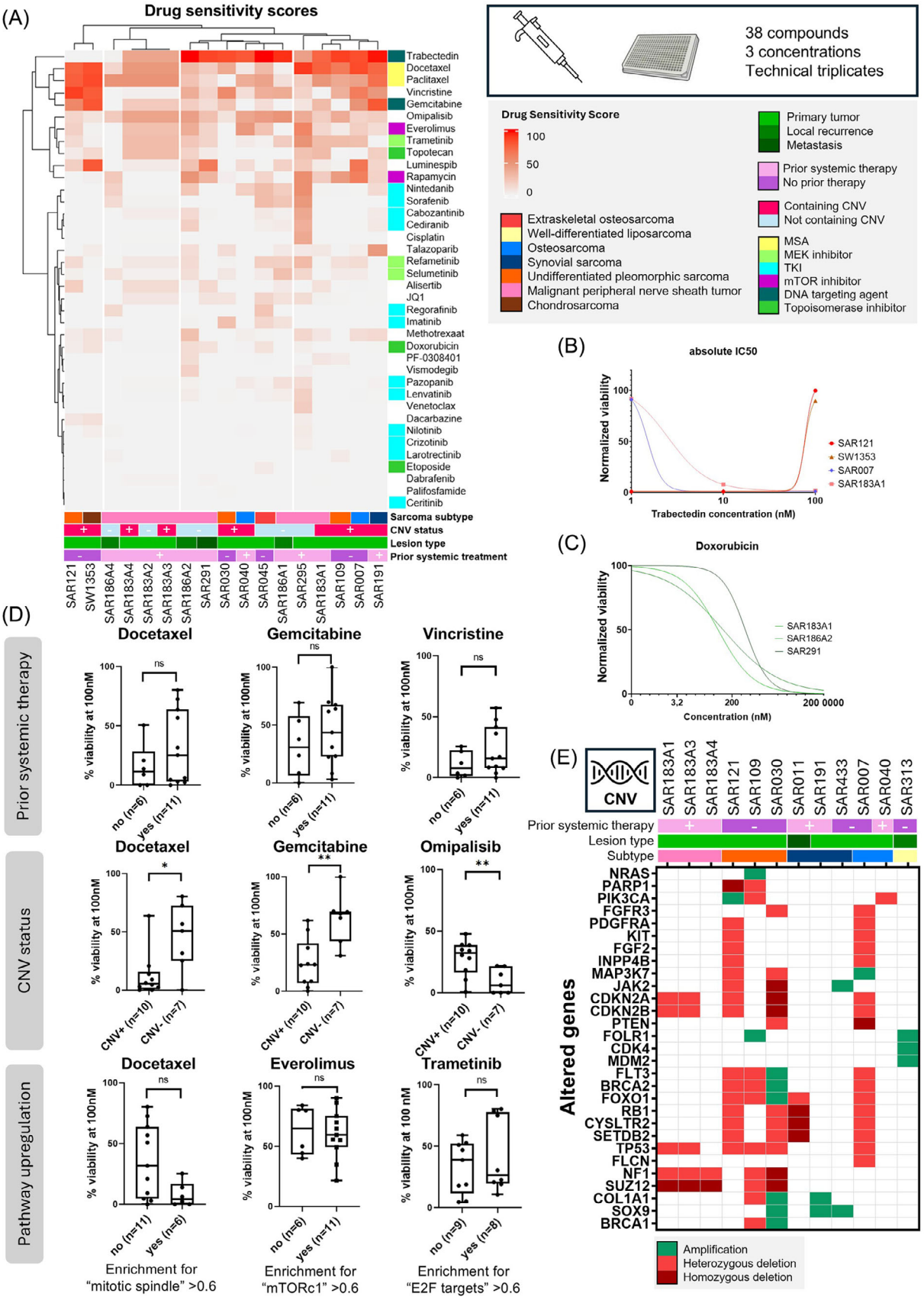

FIGURE 3 Drug sensitivity screening and correlation to biological data. (A) Hierarchical cluster analysis of drug sensitivity scores (DSS) to specified treatments, tested in technical triplicates. 38 different compounds were tested in concentrations of 1 nm, 10 and 100 nM. DSS were calculated as described by Yadav et al. [17] Hierarchical cluster analysis was performed applying agglomerative nesting, Euclidian metric and

that PDCs with CNVs exhibit higher expression of several hallmark pathways, including Hedgehog signalling, *E2F* targets and *MYC* targets (Figure 2D).

3.2 | Phenotypic drug sensitivity screening uncovers functional insights not captured by genomic or transcriptomic sequencing

A 38-compound drug panel was screened across the early-passage sarcoma PDC cultures, including agents already used clinically as well as compounds in various stages of translational development (Figure 3A). Drug sensitivity scores (DSS) revealed that the majority of PDCs were sensitive to Trabectedin. In some PDCs, the cytotoxic effect of Trabectedin was strongest at 1–10 nM but diminished at 100 nM (Figure 3B), suggesting nonlinear concentration–response behaviour in specific sarcoma subtypes. Microtubule-stabilizing agents such as Docetaxel, Paclitaxel and microtubule-destabilizing agent Vincristine clustered tightly together, consistent with their shared mechanisms of action and comparable effectiveness across sarcoma subtypes. Notably, their activity appeared independent of CNV status or lineage. The standard of care treatment Doxorubicin elicited a limited effect on the PDCs in the 1–100 nM concentration range, but showed higher efficacy at concentrations surpassing 100 nM (Figure 3C). The *PI3K* inhibitor Omipalisib and downstream *mTOR* inhibitors Everolimus and Rapamycin were also among the most effective kinase inhibitors, in agreement with ssGSEA pathway activity. By contrast, targeted agents commonly used clinically in sarcoma—such as the multikinase inhibitors Pazopanib, Regorafenib and Sorafenib—showed minimal to no activity across all PDCs tested, underscoring the limited functional impact of these TKIs in the ex vivo setting.

To explore clinical correlates of drug response, PDCs were stratified into clinically relevant subgroups and the activity of specific therapies was compared (Figure 3D). No significant differences were observed when comparing PDCs from pretreated sarcoma samples. However, PDCs harbouring CNV alterations responded more strongly to Docetaxel and Gemcitabine, the latter frequently used in combination with Docetaxel as a second-line therapy for soft tissue sarcoma. Overall, drug response evaluation demonstrates that functional phenotypic drug screening captures therapeutically relevant heterogeneity not evident from genomic or transcriptomic data alone.

3.3 | Intra-tumoural and site-specific heterogeneity captured by sarcoma patient-derived cultures

Eight cell cultures were derived from a single patient with MPNST. SAR183A1 to A4 were established from spatially distinct regions of the patient's primary tumour. SAR186A1, SAR186A2 and SAR186A4 were generated from tissue sampled at different locations within the local recurrence. SAR291 was derived from a lung metastasis obtained from the same patient (Supplementary Figure 1). The DNA of these tumour samples and their corresponding PDCs was analysed using CNV sequencing. The recurrence tissue samples of SAR186A1, SAR186A2 and SAR186A4 revealed no significant alterations in copy number and neither did their corresponding PDCs (Supplementary Figure 4). For SAR183A2 and SAR291, however, the CNVs present in the original tumour tissue were no longer detectable in the corresponding cell cultures (Figure 4G). Such loss of CNVs upon in-vitro expansion is consistent with the well-described clonal selection that occurs during cell culture establishment, where only specific subpopulations adapt and outgrow others.[4, 13] In contrast, analysis of key MPNST-related genes showed that the CNVs observed in the primary tumour were retained in the SAR183A1, SAR183A3 and SAR183A4 cultures (Figure 4G). The overall similarity of the complete CNV profiles among SAR183A1, SAR183A3 and SAR183A4 ranged from 50.7% to 78.1%. Notably, the SAR183A4 culture exhibited only a heterozygous loss of *NF1*, *CDKN2A* and *CDKN2B* copy number, whereas the original primary tumour tissue harboured homozygous deletions of these genes, indicating that cells with incomplete loss of these loci were selectively enriched during the culturing process. While many CNVs may represent passenger events without major functional consequences, all PDCs retained a common lineage signature while exhibiting transcriptomic divergence reflective of disease progression (PCA plot and hierarchical clustering, Figure 2A,C). This finding is also confirmed at the

ward linkage method. (B) Dose–response curve of trabectedin in four distinct PDCs. (C) Dose–response curve of Doxorubicin in higher concentrations than the ones tested in the high-throughput experiments. (D) Maximum effect of specific treatments in clinically relevant subgroups. PDCs were grouped into the described categories and maximum effects at 100 nM were graphed. Mann–Whitney *U* tests were performed to calculate differences between groups. (E) Copy number variations in a sarcoma-relevant subset of genes. A subset of sarcoma-relevant genes was selected from OncoKB[23] and all CNV data was cross referenced. An amplification was called at a Z-score higher than 0.35, a homozygous loss was called at a Z-score of -2 or lower and a heterozygous deletion was called at a Z-score between -0.35 and -2 (Supplementary Figure 4).

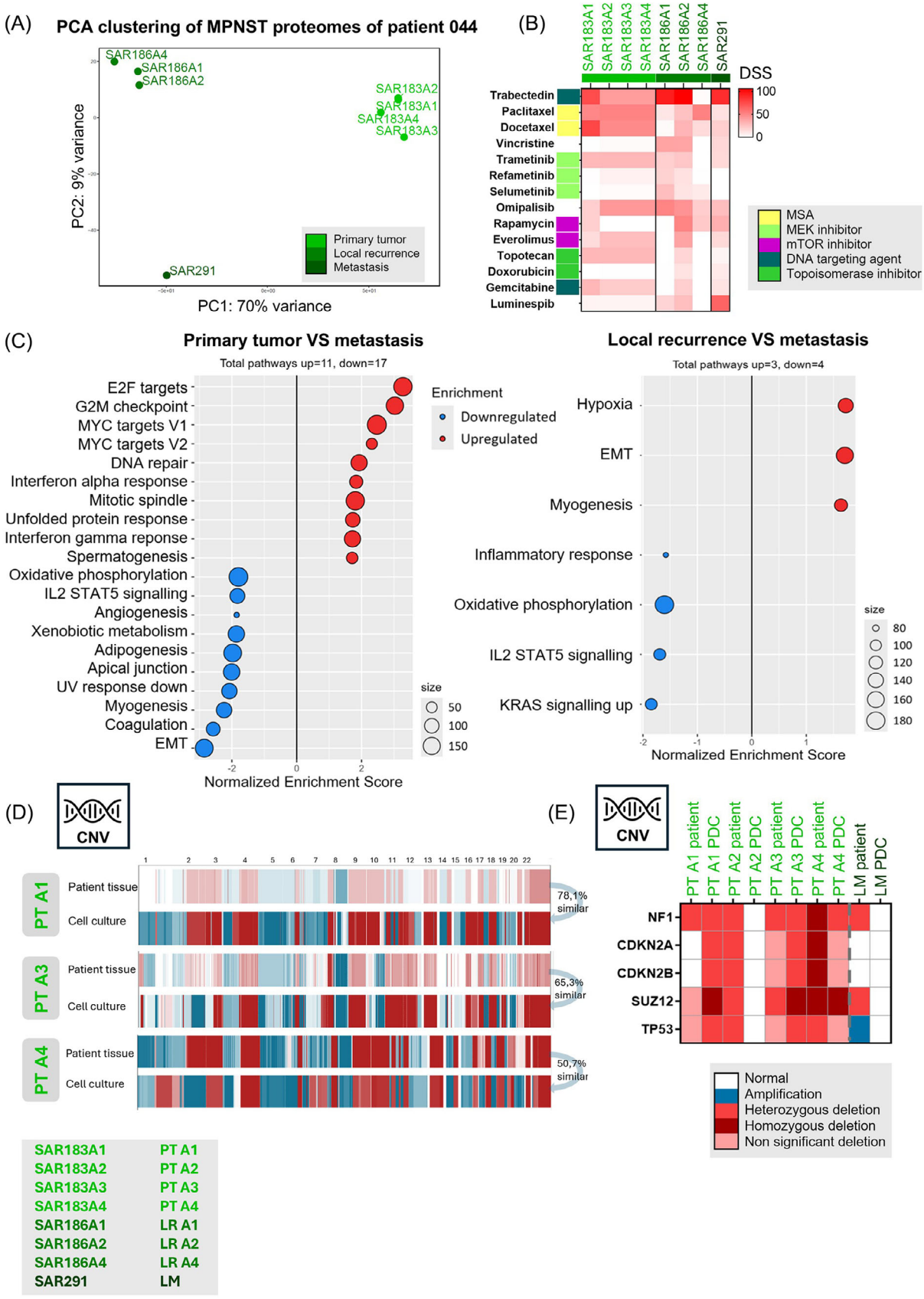

FIGURE 4 Comparison of multiple sampling locations in the primary tumour, local recurrence and lung metastasis of patient 044 (Supplementary Figure 1). (A) PCA plot of PDC proteomes. (B) Subset of DSS results of PDCs derived from distinct disease stages in the same patient. (C) GSEA of the primary tumour, local recurrence and metastasis PDCs. A *p*-value of 0.001 was applied for significance. Only the top

proteome level. PCA of the proteomic signatures resolved the cultures into three major clusters: one comprising the primary tumour samples (SAR183A1–A4), a second consisting of the local recurrence cultures (SAR186A1–A4) and a third represented by the lung metastasis culture (SAR291) (Figure 4A). Gene set enrichment analysis of the proteomic data revealed increased abundance of several targetable pathways in the PDC derived from the primary tumour compared with those from the local recurrence and metastasis, including hallmarks such as G2M checkpoint and epithelial to mesenchymal transition (Figures 4C and 5C). Consistent with these findings, drug sensitivity screening showed a higher sensitivity of the primary tumour PDC to microtubule-targeting agents such as paclitaxel and docetaxel when compared to the local recurrence or metastasis. In addition, the primary tumour derived cells exhibited overexpression of proliferative signalling pathways, including *E2F* targets and *MYC* targets, aligning with their increased sensitivity to DNA-targeting gemcitabine, and the topoisomerase inhibitor topotecan. No major differences in kinase pathway activation were detected between the primary, recurrent, and metastatic MPNST cultures, consistent with the observation that *MEK, PI3K* and *mTOR* inhibitors showed activity across all three stages, although compound-specific differences in sensitivity were apparent. Notably, the MPNST PDC culture from the metastasis showed pronounced sensitivity to HSP90 inhibition, consistent with its stronger EMT-associated transcriptional program, as cells in mesenchymal state often display increased reliance on HSP90-dependent proteostasis and signaling[37] (Figure 4B).

Given the differences observed in the proteomes of cell cultures derived from primary sarcomas versus metastatic lesions, we next examined whether these distinctions were also reflected in the EVs released by these cells. Because EVs are key mediators of intercellular communication and represent a rich source of potential biomarkers, we analysed their proteomic composition. EVs were isolated from primary tumour-, local recurrence- and metastasis-derived cultures, and their protein content was systematically profiled. A PCA of the EV proteomes showed clustering patterns similar to those of the corresponding cell cultures, with clear separation according to tumour site (Figure 5A). Because local relapse maintains direct evolutionary continuity with the primary tumour, its EV composition is better suited to identifying subtle progression-associated changes than that of the biologically distinct metastasis. To investigate this, GSEA was applied to the primary tumour and local recurrence PDCs and EVs, revealing that the differentially expressed pathways 'interferon gamma response', 'interferon alpha response' and 'MYC targets V1' in the cell cultures were also detectable in their EVs. A volcano plot further highlighted stage-specific EV signatures: the metastatic culture released EVs enriched for EMT-associated proteins—most prominently S100A4, COL1A2 and CHI3L1, together with ECM and cytoskeletal regulators such as PODN, MTCL2 and ITIH2—supporting the EV proteome as a sensitive indicator of a mesenchymal, invasion-prone cell state. In contrast, EVs from the primary tumour cultures were characterized by marked enrichment of MYC_TARGETS_V2, driven by high levels of DDX1 and additional MYC-responsive proteins, consistent with a bona fide MYC-driven proliferative program at the primary disease stage (Figure 5B). EV markers representing membrane tetraspanins (CD9, CD63, CD81), lipid raft proteins (FLOT1/2), ESCRT components (SDCBP, PDCD6IP, TSG101), vesicle trafficking regulators (Rab27A/B) and plasma membrane-derived EV biogenesis (ARRDC1) showed stable abundance with limited variability across PDC locations, indicating consistent EV production and isolation (Figure 5C).

In line with the EMT-associated proteomic differences observed between primary tumour-derived and relapse-derived cultures, we next assessed cellular morphology in 2D and invasive behaviour in 3D type I collagen matrices. Quantification of cell area, perimeter, circularity, and roundness followed by PCA revealed distinct morphological clustering between primary tumour and local relapse PDC cultures (Figure 5E), indicating a shift toward a more mesenchymal morphometric profile in the relapse-derived cells. Consistently, invasion assays using 3D type I collagen gels demonstrated that two out of three local relapse cultures exhibited markedly greater invasive capacity compared to all primary cultures, as reflected by significantly increased invasion area measured from spheroids (Figure 5F). Together, these findings support that relapse-derived MPNST cultures acquire mesenchymal morphotype with enhanced invasive potential compared with their primary tumour counterparts.

4 | DISCUSSION

In this study, we established and comprehensively characterized a panel of early-passage PDC cultures representing eleven distinct sarcoma subtypes. By integrating genomic,

10 significant up- and downregulated pathways are shown. (D) Direct comparisons of CNV profiles of patient samples with their corresponding PDCs. Similarities were calculated with the CNpare package in R.[24] (E) Comparison of CNV in a MPNST-relevant subset of genes between patient tissue and PDC. Genes were selected based on publications in MPNST and OncoKB.[1, 23, 33] An amplification was called at a *Z*-score of more than 0.35, and a loss was called at a *Z*-score of less than 0.35 (Supplementary Figure 4).

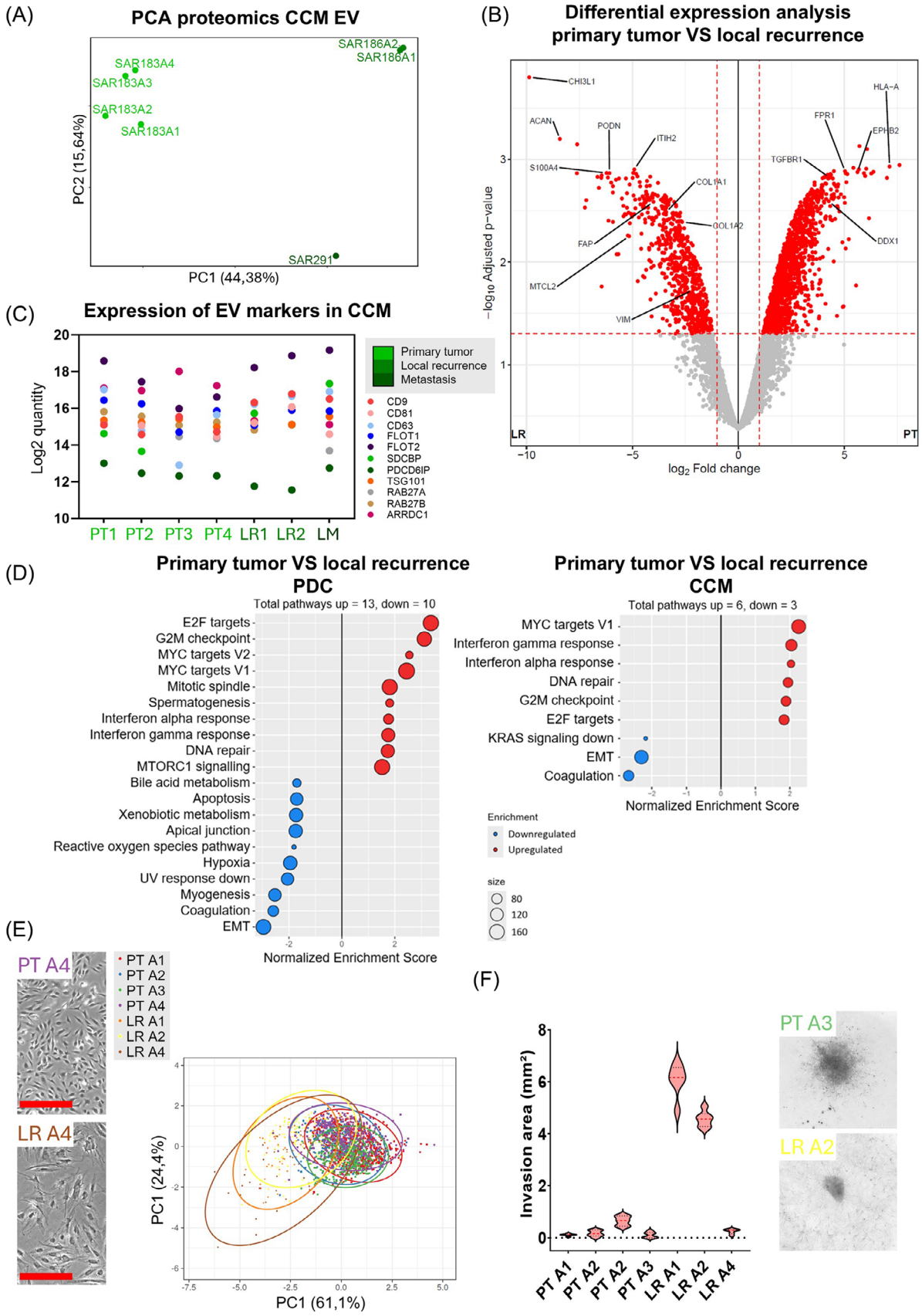

FIGURE 5 Extracellular vesicle (EV) and functional analysis from multiple tumour locations in patient 044. (A) PCA clustering of the proteomes from EVs isolated from CCM of the corresponding PDCs. (B) The volcano plot based on CCM derived EVs shows differential expression of several mesenchymal markers when comparing the primary tumour CCM EVs to the local recurrence CCM EVs. (C) Expression

transcriptomic, proteomic, EV profiling, morphological analysis and functional drug sensitivity screening, we demonstrate that these models recapitulate key molecular features of their tumours of origin and capture clinically and biologically meaningful heterogeneity across sarcoma lineages and disease stages. In accordance with others, our findings collectively underscore the value of early-passage PDCs as tumour relevant models for dissecting sarcoma biology and informing functional precision medicine.[38]

The successful derivation of 29 PDC cultures from 19 patients spanning a broad clinical spectrum reflects the feasibility of establishing stable, early-passage sarcoma models from diverse histologies, including both relatively frequent sarcoma subtypes (MPNST, UPS, MFS, SS, LMS) and rarer entities (*BCOR*-altered sarcoma, EOS, RMS). Morphologically, most cultures adopted the spindle-like appearance classically associated with mesenchymal tumours, while suspended cell pellets consistently displayed the enlarged nuclear-to-cytoplasmic ratio characteristic of malignant cells. These observations support that early-passage cultures retain core cytological features of their respective sarcomas.[39–41] Given the marked heterogeneity of sarcomas, these findings cannot be generalized across the full spectrum of sarcoma subtypes. Nevertheless, they highlight the value of functional screening as a complementary approach that can reveal therapeutic vulnerabilities beyond those identified through multi-omic profiling alone.

Genomic analysis further confirmed preservation of tumour-associated alterations. CNV profiling identified recurrent losses of *CDKN2A/B* and *NF1*, particularly amongst MPNST cultures, in line with known pathogenic drivers of this disease. SS cultures consistently exhibited a shared amplification on chromosome 17, suggesting a selective advantage maintained during in vitro expansion. UPS cultures displayed the most complex genomic landscapes, consistent with their highly rearranged genomes in vivo. Importantly, although some CNVs present in the original tumour tissue were not retained in culture—particularly in samples undergoing clonal bottlenecks or selection—each PDC conserved a subset of biologically relevant CNVs, especially those related to sarcoma lineage identity or tumour progression. These observations highlight the dynamic interplay between selective pressures during culture establishment and the preservation of tumour-defining genomic features also observed in other tumour entities.[42]

At the transcriptomic level, PCA and hierarchical clustering analyses revealed pronounced lineage-specific segregation of sarcoma PDCs, consistent with previously published sarcoma organoid cultures.[38] Fusion-driven entities such as SS formed tightly clustered, isolated groups, reflecting their coherent and characteristic transcriptional programs. Conversely, complex-karyotype sarcomas, including MFS and UPS, also formed distinct subtype-specific clusters, with UPS cultures demonstrating a more dedifferentiated, transcriptionally divergent identity. LMS cultures clustered together, maintaining smooth muscle-associated signatures, while osteosarcoma and carcinosarcoma cultures occupied intermediate positions consistent with mixed or partially retained differentiation programs. Other subtypes such as LPS, RMS, GCT and *BCOR*-altered sarcoma mapped to unique transcriptomic spaces aligned with their known biology. These findings underscore that lineage of origin is a major determinant of transcriptional architecture in sarcoma PDCs.

The MPNST cultures, derived from spatially distinct regions of a primary tumour, a local recurrence and a distant metastasis, provided a powerful opportunity to examine patterns of intra-tumoural and inter-site heterogeneity. Transcriptomic and proteomic PCA clearly separated primary, relapse and metastatic cultures, supporting the concept that disease progression is accompanied by increasingly divergent biological states and in agreement with others work.[43] Although all MPNST cultures retained hallmark lineage-defining features, relapse-derived cultures displayed enrichment of EMT-associated transcriptional programs accompanied by increased invasive capacity, while the metastatic culture exhibited the most pronounced EMT-like state and a distinct sensitivity to HSP90 inhibition. In mesenchymal malignancies such as sarcomas, this EMT-like state does not represent a literal epithelial-to-mesenchymal transition but rather reflects activation of conserved transcriptional programs that drive mesenchymal plasticity, cytoskeletal remodelling, and invasive behaviour. HSP90-targeted strategies have been evaluated clinically in sarcomas, including an MPNST-enriched study of ganetespib plus the mTOR

of EV markers in CCM derived from PDCs shows stable expression of membrane tetraspanins, lipid raft proteins, ESCRT components, vesicle traffic regulators and plasma membrane-derived EV biogenesis makers. (D) GSEA of proteomic data comparing primary tumour to local recurrence in both PDCs, and CCM EVs derived from the corresponding PDCs. Only the top 10 signficant pathways are shown. A p-value of 0.001 was applied. (E) PCA plot of PDC phenotypes based on circularity, area, perimeter and roundness of the cells as measured with fluorescence microscopy. Every point is a measured cell. Representative images are shown (Scale bar = 50 μm). (F) Results of collagen invasion assay of the PDC reveals significant differences in invasive capacity of PDCs derived from the same patient. Six technical replicates per condition were included. Differences were calculated with a Kruskal–Wallis test with Dunn's correction for multiple comparisons, showing a significant difference ($p < 0.0001$). Representative images (magnification ×4) are shown.

inhibitor sirolimus (SARC023; NCT02008877), but objective responses in unselected MPNST were not observed.[44] In contrast, activity of HSP90 inhibition in molecularly defined sarcoma settings (e.g., KIT/PDGFRA-driven GIST) supports the rationale that biomarker-selected metastatic MPNST subsets may derive greater benefit from HSP90-directed therapy.[45]

Together, these data illustrate the value of PDCs for capturing progression-related phenotypes that cannot be inferred from bulk tumour sequencing alone. To further support the relevance of PDC cultures, ssGSEA identified pathways that were reproducibly enriched across most sarcoma PDCs, independent of histologic subtype. *MYC* targets, *TGF-β* signalling, oxidative phosphorylation and *mTORC1* signalling were consistently activated, suggesting convergent biological dependencies across distinct sarcoma lineages in agreement with Tsherniak et al. [46]

Functional drug sensitivity screening demonstrated that PDCs serve as robust platforms for identifying therapeutically relevant vulnerabilities, many of which were not predictable from genomic or transcriptomic data alone. Consistent with clinical observations, most PDCs were sensitive to trabectedin, although several displayed non-linear dose–response relationships that may reflect subtype-specific pharmacodynamics. Microtubule-targeting agents such as docetaxel, paclitaxel and vincristine showed broad efficacy across sarcoma lineages and clustered together in sensitivity analyses, reflecting conserved mechanisms of action. Kinase inhibitors targeting the PI3K–mTOR axis were among the most effective targeted agents, in agreement with pathway enrichment detected by ssGSEA. In contrast, multikinase inhibitors widely used in sarcoma treatment, including pazopanib, regorafenib and sorafenib, demonstrated limited activity ex vivo, highlighting a disconnection between pathway activation signatures and therapeutic response that warrants further investigation.[9] A key limitation is the absence of an appropriate non-malignant comparator. Because the cell of origin of many sarcoma subtypes remains incompletely defined, selecting a biologically relevant control culture is challenging. Moreover, the marked heterogeneity across sarcoma histologies makes any single non-tumour comparator unlikely to represent a meaningful reference for all models studied.[47]

Given the molecular and phenotypic divergence observed between PDCs derived from primary tumours, local recurrences and metastases, we examined whether such differences were also reflected in their secreted EV. Proteomic analysis of EVs mirrored the clustering patterns identified in cell-based analyses, supporting the use of EVs as non-invasive indicators of tumour evolution. EVs from primary tumour cultures exhibited enrichment of MYC_TARGETS_V2, driven by high levels of *DDX1* and other *MYC*-responsive proteins, consistent with a proliferative phenotype. EVs derived from relapse cultures captured increased mesenchymal and matrix-remodelling signatures, paralleling their transcriptomic and morphological profiles. These stage-specific EV signatures highlight the potential of EV profiling to monitor disease progression and identify biologically meaningful transitions in tumour state confirming extensive work done using plasma-derived EV signatures.[48]

Together, these findings demonstrate that early-passage sarcoma PDCs faithfully preserve lineage identity, progression-related phenotypes, and functional therapeutic vulnerabilities. The integration of multi-omic and phenotypic profiling provides a rich framework to study sarcoma biology, identify actionable dependencies, and develop personalized treatment strategies grounded in the functional behaviour of PDC cultures.

AUTHOR CONTRIBUTIONS

Stefanie Gijsels: Conceptualization; methodology; validation; formal analysis; investigation; data curation; writing–original draft; writing–review and editing; visualization; project administration. **Suzanne Fischer**: Conceptualization; methodology; investigation; writing–review and editing; project administration; funding acquisition. **David Creytens**: Conceptualization; methodology; resources; writing–review and editing; supervision. **Sándor Dedeyne**: Methodology; software; formal analysis; data curation. **Felix De Vuyst**: Methodology; investigation; draft; writing–review and editing. **Cláudio Pinheiro**: Methodology; investigation; writing–review and editing. **Fleur Cordier**: Methodology; resources; writing–review and editing; visualization; supervision. **Sarah-Lee Bekaert**: Methodology; software; validation; formal analysis; writing–review and editing; visualization. **Nadine Van Roy**: Methodology; software; resources; writing–review and editing; supervision. **Kaat Durinck**: Methodology; software; resources; writing–review and editing; supervision. **Jarne Pauwels**: Methodology; software; formal analysis; resources; data curation; writing–review and editing. **Kris Gevaert**: Software; resources; writing–review and editing; supervision. **Pieter Mestdagh**: Methodology; software; resources; writing–review and editing; supervision. **Jo Vandesompele**: Methodology; software; resources; writing–review and editing; supervision. **Pekka Rappu**: Methodology; software; formal analysis; data curation; resources; writing–review and editing. **Jyrki Heino**: Methodology; software; resources; writing–review and editing; supervision. **An Hendrix**: Resources; writing–review and editing; supervision; funding acquisition. **Gabrielle H. van Ramshorst**: Resources; writing–review and editing; supervision. **Gwen Sys**: Resources; writing–review and

editing; supervision; project administration; funding acquisition. **Olivier De Wever**: Conceptualization; methodology; resources; writing–original draft; writing–review and editing; supervision; project administration; funding acquisition.

ACKNOWLEDGEMENTS

Mass spectrometry analyses for EV proteomics were performed at the Turku Proteomics Facility, supported by Biocenter Finland. This study was supported by the Cancer Research Institute Ghent, Stichting Tegen Kanker (2022-147) and Kom op tegen Kanker (A18/OC/0303). David Creytens was financially supported by a senior clinical research fellowship from the Research Foundation Flanders (FWO) (1800725N).

ETHICS STATEMENT

Patients with suspected sarcoma were included after written informed consent (EC 2018/0080 and EC/2019/0178) by the Ghent University Hospital Ethical Committee. The study was performed in accordance with the Declaration of Helsinki.

ORCID

Stefanie Gijsels https://orcid.org/0000-0003-3742-5160
Cláudio Pinheiro https://orcid.org/0000-0003-1834-199X
Jo Vandesompele https://orcid.org/0000-0001-6274-0184

REFERENCES

1. WHO classification of tumours editorial board. *WHO Classification of Tumours: Soft Tissue and Bone Tumours*. 5th ed. Vol. 3. World Health Organization; 2020.
2. Gatta G, Capocaccia R, Botta L, et al. Burden and centralised treatment in Europe of rare tumours: results of RARECAREnet—a population-based study. *Lancet Oncol*. 2017;18(8):1022-1039. doi:10.1016/S1470-2045(17)30445-X
3. Amon A, Androgé C, Asselman L, et al. Belgian Cancer Registry: Bone & Soft Tissue Tumour Epidemiology in Belgium 2004–2019. Cancer Incidence in Belgium. 2022.
4. van Staveren WCG, Solís DYW, Hébrant A, Detours V, Dumont JE, Maenhaut C. Human cancer cell lines: experimental models for cancer cells in situ? For cancer stem cells? *Biochim Biophys Acta Rev Cancer*. 2009;1795(2):92-103. doi:10.1016/j.bbcan.2008.12.004
5. Ibarrola-Villava M, Cervantes A, Bardelli A. Preclinical models for precision oncology. *Biochim Biophys Acta Rev Cancer*. 2018;1870(2):239-246. doi:10.1016/j.bbcan.2018.06.004
6. Pan X, Yoshida A, Kawai A, Kondo T. Current status of publicly available sarcoma cell lines for use in proteomic studies. *Expert Rev Proteomics*. 2016;13(2):227-240. doi:10.1586/14789450.2016.1132166
7. Grünewald TG, Alonso M, Avnet S, et al. Sarcoma treatment in the era of molecular medicine. *EMBO Mol Med*. 2020;12(11):e11131. doi:10.15252/emmm.201911131
8. Mackall CL, Meltzer PS, Helman LJ. Focus on sarcomas. *Cancer Cell*. 2002;2(3):175-178. doi:10.1016/S1535-6108(02)00132-0
9. Gronchi A, Miah AB, Dei Tos AP, et al. Soft tissue and visceral sarcomas: eSMO–EURACAN–GENTURIS Clinical Practice Guidelines for diagnosis, treatment and follow-up☆. *Ann Oncol*. 2021;32(11):1348-1365. doi:10.1016/j.annonc.2021.07.006
10. Yang W, Soares J, Greninger P, et al. Genomics of Drug Sensitivity in Cancer (GDSC): a resource for therapeutic biomarker discovery in cancer cells. *Nucleic Acids Res*. 2013;41(D1):D955-D961. doi:10.1093/NAR/GKS1111
11. Tlemsani C, Heske CM, Elloumi F, et al. Sarcoma_CellminerCDB: a tool to interrogate the genomic and functional characteristics of a comprehensive collection of sarcoma cell lines. *iScience*. 2024;27(6):109781. doi:10.1016/J.ISCI.2024.109781
12. Bahia H, Ashman JNE, Cawkwell L, et al. Karyotypic variation between independently cultured strains of the cell line MCF-7 identified by multicolour fluorescence in situ hybridization. *Int J Oncol*. 2002;20:489-494.
13. Ben-David U, Siranosian B, Ha G, et al. Genetic and transcriptional evolution alters cancer cell line drug response. *Nature*. 2018;560(7718):325-330. doi:10.1038/s41586-018-0409-3
14. Cho YE, Kim SC, Kim HJ, Han I, Ku JL. Establishment and characterization of 18 sarcoma cell lines: unraveling the molecular mechanisms of doxorubicin resistance in sarcoma cell lines. *J Transl Med*. 2024;22(1):889. doi:10.1186/s12967-024-05700-y
15. Kolberg M, Bruun J, Murumägi A, et al. Drug sensitivity and resistance testing identifies PLK1 inhibitors and gemcitabine as potent drugs for malignant peripheral nerve sheath tumors. *Mol Oncol*. 2017;11(9):1156-1171. doi:10.1002/1878-0261.12086
16. Gijsels S, Vekeman M, Fischer S, et al. Preserving potential: surgeons as key partners in establishing a living sarcoma biobank for translational research purposes. *Surg Oncol*. 2025;59:102209. doi:10.1016/j.suronc.2025.102209
17. Yadav B, Pemovska T, Szwajda A, et al. Quantitative scoring of differential drug sensitivity for individually optimized anticancer therapies. *Sci Rep*. 2014;4(1):5193. doi:10.1038/srep05193
18. Metsalu T, Vilo J. ClustVis: a web tool for visualizing clustering of multivariate data using principal component analysis and heatmap. *Nucleic Acids Res*. 2015;43(W1):W566-W570. doi:10.1093/nar/gkv468
19. Liberzon A, Birger C, Thorvaldsdóttir H, Ghandi M, Mesirov JP, Tamayo P. The molecular signatures database hallmark gene set collection. *Cell Syst*. 2015;1(6):417-425. doi:10.1016/J.CELS.2015.12.004
20. Scheinin I, Sie D, Bengtsson H, et al. DNA copy number analysis of fresh and formalin-fixed specimens by shallow whole-genome sequencing with identification and exclusion of problematic regions in the genome assembly. *Genome Res*. 2014;24(12):2022-2032. doi:10.1101/GR.175141.114
21. Sante T, Vergult S, Volders PJ, et al. ViVar: a comprehensive platform for the analysis and visualization of structural genomic variation. *PLoS One*. 2014;9(12):e113800. doi:10.1371/JOURNAL.PONE.0113800
22. Suehnholz SP, Nissan MH, Zhang H, et al. Quantifying the expanding landscape of clinical actionability for patients with cancer. *Cancer Discov* 2024;14(1):49-65. doi:10.1158/2159-8290.CD-23-0467/3372948/CD-23-0467.PDF
23. Chakravarty D, Gao J, Phillips S, et al. OncoKB: a precision oncology knowledge base. *JCO Precis Oncol*. 2017;(1):1-16. doi:10.1200/PO.17.00011/SUPPL_FILE/DS_17.00011.DOCX

24. Chaves-Urbano B, Hernando B, Garcia MJ, Macintyre G. CNpare: matching DNA copy number profiles. *Bioinformatics*. 2022;38(14):3638-3641. doi:10.1093/BIOINFORMATICS/BTAC371
25. Van Deun J, Mestdagh P, Sormunen R, et al. The impact of disparate isolation methods for extracellular vesicles on downstream RNA profiling. *J Extracell Vesicles*. 2014;3(1):24858. doi:10.3402/JEV.V3.24858
26. Roux Q, Boiy R, De Vuyst F, et al. Depletion of soluble cytokines unlocks the immunomodulatory bioactivity of extracellular vesicles. *J Extracell Vesicles*. 2023;12(8):e12339. doi:10.1002/JEV2.12339
27. Roux Q, Deville S, Hendrix A. Density-based Fractionation of cell-conditioned medium to prepare proteomics grade extracellular vesicles. *Methods Mol Biol*. 2023;2718:253-269. doi:10.1007/978-1-0716-3457-8_14
28. Vergauwen G, Dhondt B, Van Deun J, et al. Confounding factors of ultrafiltration and protein analysis in extracellular vesicle research. *Sci Rep*. 2017;7(1):2407. doi:10.1038/S41598-017-02599-Y
29. Van Deun J, Mestdagh P, Agostinis P, et al. EV-TRACK: transparent reporting and centralizing knowledge in extracellular vesicle research. *Nat Methods*. 2017 14:3. 2017;14(3):228-232. doi:10.1038/nmeth.4185
30. Wiśniewski JR, Zougman A, Nagaraj N, Mann M. Universal sample preparation method for proteome analysis. *Nat Methods*. 2009;6(5):359-362. doi:10.1038/NMETH.1322;KWRD
31. Dhondt B, Geeurickx E, Tulkens J, et al. Unravelling the proteomic landscape of extracellular vesicles in prostate cancer by density-based fractionation of urine. *J Extracell Vesicles*. 2020;9(1):1736935. doi:10.1080/20013078.2020.1736935
32. Dhondt B, Pinheiro C, Geeurickx E, et al. Benchmarking blood collection tubes and processing intervals for extracellular vesicle performance metrics. *J Extracell Vesicles*. 2023;12(5):e12315. doi:10.1002/jev2.12315
33. Frankenfield AM, Ni J, Ahmed M, Hao L. Protein contaminants matter: building universal protein contaminant libraries for DDA and DIA proteomics. *J Proteome Res*. 2022;21(9):2104-2113. doi:10.1021/ACS.JPROTEOME.2C00145
34. Callister SJ, Barry RC, Adkins JN, et al. Normalization approaches for removing systematic biases associated with mass spectrometry and label-free proteomics. *J Proteome Res*. 2006;5(2):277–286. doi:10.1021/pr0503001
35. Cortes-Ciriano I, Steele CD, Piculell K, et al. Genomic patterns of malignant peripheral nerve sheath tumor (MPNST) evolution correlate with clinical outcome and are detectable in cell-free DNA. *Cancer Discov*. 2023;13(3):654-671. doi:10.1158/2159-8290.CD-22-0786/712001/AM/GENOMIC-PATTERNS-OF-MALIGNANT-PERIPHERAL-NERVE
36. Feng X, Pleasance E, Zhao EY, et al. Therapeutic implication of genomic landscape of adult metastatic sarcoma. *JCO Precis Oncol*. 2019;(3):1-25. doi:10.1200/PO.18.00325/ASSET/979ED3BD-96AB-4B45-9AB4-FA4D949A2790/ASSETS/IMAGES/LARGE/PO.18.00325TA4.JPG
37. Lamouille S, Xu J, Derynck R. Molecular mechanisms of epithelial-mesenchymal transition. *Nat Rev Mol Cell Biol*. 2014;15(3):178-196. doi:10.1038/NRM3758
38. Al Shihabi A, Tebon PJ, Nguyen HTL, et al. The landscape of drug sensitivity and resistance in sarcoma. *Cell Stem Cell*. 2024;31(10):1524-1542.e4. doi:10.1016/j.stem.2024.08.010
39. Coward VS, Dorsey J, Babichev Y, et al. Optimal factors that influence the establishment of successful primary human soft-tissue sarcoma cell lines. *Clin Can Res*. 2025;31(18):3984-3993. doi:10.1158/1078-0432.CCR-25-0111
40. Salawu A, Fernando M, Hughes D, et al. Establishment and molecular characterisation of seven novel soft-tissue sarcoma cell lines. *Br J Cancer*. 2016;115(9):1058-1068. doi:10.1038/bjc.2016.259
41. Hu M, Nicolson GL, Trent JC, Yu D, Zhang L, Lang A, et al. Characterization of 11 human sarcoma cell strains: evaluation of cytogenetics, tumorigenicity, metastasis, and production of angiogenic factors. *Cancer*. 2002;95(7):1569-1576. REQUESTEDJOURNAL:JOURNAL:10970142;WGROUP:STRING:PUBLICATION PubMed PMID: 12237927. doi:10.1002/CNCR.10879
42. Raghavan S, Winter PS, Navia AW, et al. Microenvironment drives cell state, plasticity, and drug response in pancreatic cancer. *Cell*. 2021;184(25):6119-6137.e26. doi:10.1016/j.cell.2021.11.017
43. Fang Y, Elahi A, Denley RC, Rao PH, Brennan MF, Jhanwar SC. Molecular characterization of permanent cell lines from primary, metastatic and recurrent malignant peripheral nerve sheath tumors (MPNST) with underlying neurofibromatosis-1. *Anticancer Res*. 2009;29(4):1255-1262.
44. Kim A, Lu Y, Okuno SH, et al. Targeting refractory sarcomas and malignant peripheral nerve sheath tumors in a phase I/II study of sirolimus in combination with ganetespib (SARC023). *Sarcoma*. 2020;2020:1-8. doi:10.1155/2020/5784876
45. Kurokawa Y, Honma Y, Sawaki A, et al. Pimitespib in patients with advanced gastrointestinal stromal tumor (CHAPTER-GIST-301): a randomized, double-blind, placebo-controlled phase III trial. *Ann Oncol*. 2022;33(9):959-967. doi:10.1016/j.annonc.2022.05.518
46. Tsherniak A, Vazquez F, Montgomery PG, et al. Defining a cancer dependency map. *Cell*. 2017;170(3):564-576.e16. doi:10.1016/j.cell.2017.06.010
47. Damerell V, Pepper MS, Prince S. Molecular mechanisms underpinning sarcomas and implications for current and future therapy. *Signal Transduct Target Ther*. 2021;6(1):1-19. doi:10.1038/S41392-021-00647-8;SUBJMETA
48. Hoshino A, Kim HS, Bojmar L, et al. Extracellular vesicle and particle biomarkers define multiple human cancers. *Cell*. 2020;182(4):1044-1061.e18. doi:10.1016/j.cell.2020.07.009

SUPPORTING INFORMATION

Additional supporting information can be found online in the Supporting Information section at the end of this article.

How to cite this article: Gijsels S, Fischer S, Creytens D, et al. A living biobank of sarcoma patient-derived cell cultures reveals multi-omic and functional insights that capture disease heterogeneity. *Clin Transl Med*. 2026;16:e70722. https://doi.org/10.1002/ctm2.70722